Broad-Band Noise Mechanisms and Noise Measurements of Metal–Semiconductor Junctions

A. JELENSKI, MEMBER, IEEE, ERIK L. KOLLBERG, SENIOR MEMBER, IEEE, AND HERBERT H. G. ZIRATH, STUDENT MEMBER, IEEE

Abstract —Classic work on optimized heterodyne receivers has concentrated on the network aspects of mixers with limited emphasis on device properties. We present experimental results of GaAs Schottky-barrier diode noise measurements in the frequency range from 0.1 to 88 GHz and a detailed analysis of noise generation in these diodes which can explain the observed current and frequency dependence.

I. Introduction

WORK ON low-noise receiver front ends built with metal–semiconductor junctions has reached a plateau in recent years because improvements in device structures and circuit configurations seemed to be exhausted. In previous papers [1]–[6], we reported results obtained from extensive measurements performed on a number of GaAs Schottky-barrier diodes. These measurements demonstrated that in most of the diodes the measured $I-V$ and noise characteristics differ from those predicted by simple expressions based on thermionic emission and/or tunneling transport mechanisms.

It was also shown that the noise performance achieved in practical applications is mainly governed by excess noise, i.e., noise mechanisms which are not caused by classic shot and thermal noise. The observation of excess noise at low currents is consistent with a diode model describing the junction as a cluster of parallel subdiodes with different barrier heights. The details of this cluster model are discussed in [1].

In this paper, we discuss the fundamental mechanisms which affect the nonlinear current–voltage characteristics and broad-band noise properties of homogeneous GaAs barrier diodes. After a brief discussion of performed experiments and existing theories of $I-V$ and noise characteristics, it is shown that they do not accurately explain results from measurements over a wide frequency and current range. Different sources of the excess diode noise are discussed, and a more general expression for the diode noise temperature including these sources is proposed.

Manuscript received August 26, 1985; revised April 30, 1986. This work was supported in part by the Swedish Board for Technical Development.

A. Jelenski is with the University of Massachusetts, Amherst, on leave from the Institute of Electron Technology CEMI, Warsaw, Poland.

E. L. Kollberg and H. Zirath are with Chalmers University of Technology, Gothenburg, Sweden.

IEEE Log Number 8610286.

The improved model of the GaAs Schottky diode takes into account the variation of the diode effective junction temperature with the bias voltage and such components of the excess noise as hot-electron noise and frequency-dependent, trap-like noise in the junction. This model describes more accurately the observed diode noise properties over a wide range of currents and frequencies. Its utilization gives a better agreement between measured and calculated noise performances of microwave and millimeter-wave mixers [29].

Our studies are also applicable to GaAs FET's and HEMT's, where similar mechanisms of noise generation occur, as discussed by Sah [7], Baechtold [8], Pinsard [9], and Maracas [10].

II. Experimental Results

In order to investigate experimentally the sources of excess noise, a number of GaAs diodes fabricated by both university laboratories and industry were tested at dc, at frequencies from 0.1 to 88 GHz, and at temperatures from 20 to 300 K [1]–[6], [13]. The junctions were electroplated Pt-GaAs Schottky diodes and single-crystal Al-GaAs devices fabricated on vapor-phase epitaxial and MBE material. The epitaxial layers had a thickness of 0.05–0.50 μm and doping concentrations of 1×10^{16} to $2\times10^{17}\,\text{cm}^{-3}$, and the junctions had diameters of 1–3 μm.

The low ideality factors at low currents measured at room temperature for all the diodes used in our investigations ($\eta \leqslant 1.2$) prove that the material quality and the anode formation were satisfactorily controlled. This statement is further supported by the fact that the measured noise properties of the diodes can be rather fully explained within the model framework presented in this paper.

$I-V$ characteristics were measured in the temperature range from 4 to 300 K. The effective junction temperature θ (or the diode ideality factor $\eta=\theta/T$) and diode series resistance were determined from these measurements as described in [1] and [30]. A number of millimeter wave and commercially available microwave diodes were also measured in an automatic system [26], [28], giving directly graphs of $I-V$, $\eta-I$, and R_s-I relations, such as that shown in Fig. 5.

0018-9480/86/1100-1193$01.00

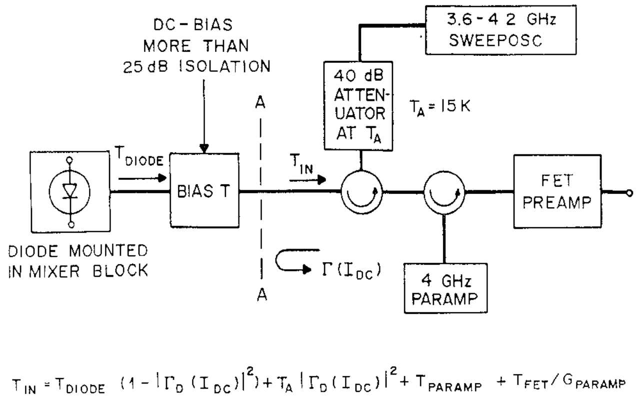

Fig. 1. Schematic view of the test apparatus for performing noise measurements at 4 GHz.

A schematic view of the test apparatus for performing the noise measurements at 4 GHz is shown in Fig. 1. A similar arrangement with low-noise FET amplifiers at lower frequencies and a mixer receiver at 17.5 GHz and 88 GHz were used. A separate low-power measurement of the reflection coefficients of the diodes was made to determine the ac differential conductance of the diode. The formula from which diode noise temperature was calculated is given in Fig. 1.

III. The Current–Voltage Characteristic

The current–voltage characteristics of an idealized and a real Schottky diode are shown schematically in Fig. 2. The real characteristic is given by [11]

$$I = I_s \exp\{(q(V - IR_s)/(k\theta)\} \tag{1}$$

where I_s is the saturation current, R_s the series resistance, q the charge of the electron, k the Boltzmann constant, and θ the effective junction temperature, which depends on the physical temperature T_0 of the junction and the electron transport mechanism across the barrier. The effective junction temperatures, or slope parameters, for the three possible means of electron transport are listed in Fig. 3. In this figure, N_D is the doping concentration of the epilayer, $\hbar$ is the Planck constant over $2\pi, \epsilon_r\epsilon_0$ is the dielectric constant of the semiconductor, m^* is the effective mass of the electron, and q is the electron charge. Thermionic emission is dominant at room temperature and thermionic-field emission at lower temperatures; at 20 K and below, field emission (tunneling) determines the diode current. It has been shown [11] that, in this case, tunneling results in an effective temperature θ which is substantially higher than the physical device temperature. This sets a limit on the minimum noise temperature which can be achieved by cooling the diode.

The formulas in Fig. 3. and (1) predict an exponential current–voltage dependance with θ independent of current for all three mechanisms. Measurements show that, in general, both the slope parameter θ and the diode noise temperature T_n vary in the investigated current range. Hence, for most diodes (but not all), the effective junction temperature θ (slope parameter) is a function of the diode

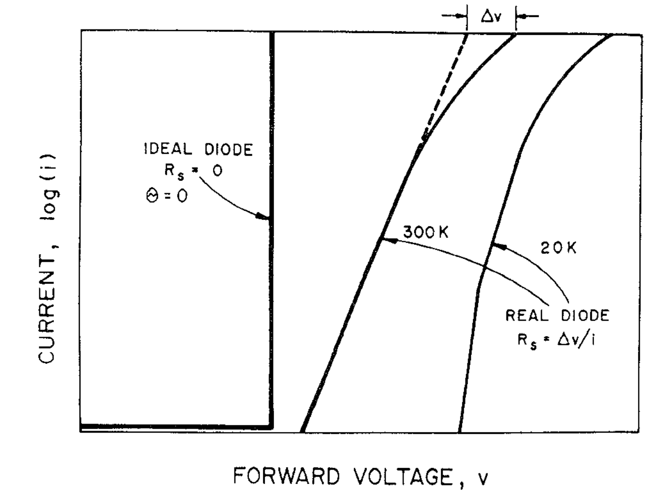

Fig. 2. Current versus voltage characteristics.

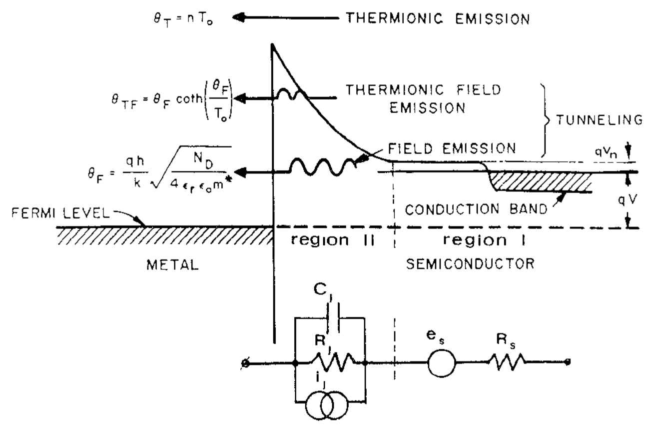

Fig. 3. Electron transport mechanisms through a metal–semiconductor junction.

current. Typical results calculated from the slope of the $\log I(V)$ characteristic using

$$\theta = (qI/k)(dV/dI) \tag{2}$$

are shown in Fig. 4 as a function of temperature. At low temperatures, where the field emission determines the current (nearly horizontal lines in Fig. 4), the value of θ increases with current in a way that is similar to its increase with epilayer doping (N_D). At high temperatures also, an increase of θ with current can be seen, as presented in Fig. 5, which gives a typical result of the ideality factor's $n(I)$ current dependence for a well-behaved diode. This figure shows that characteristics for $n(I)$ or $\theta(I)$ in the current range where the influence of the series resistance can be neglected (1–100 μA for the presented diode) are well described by the formula [26]

$$\theta(I) = \theta_0 + \theta_1(I), \qquad \text{with } \theta_1(I) = \theta_1 \cdot \ln\left(\frac{I}{I_0}\right). \tag{3}$$

At room temperatures, with $I_0 = 1\ \mu$A for the majority of the measured diodes, θ_0 was 330–375 K and typical values of θ_1 were 5–15 K for millimeter wave diodes; for microwave diodes, $\theta_0 = 300$–330 K and $\theta_1 = 2.5$–4 K. For

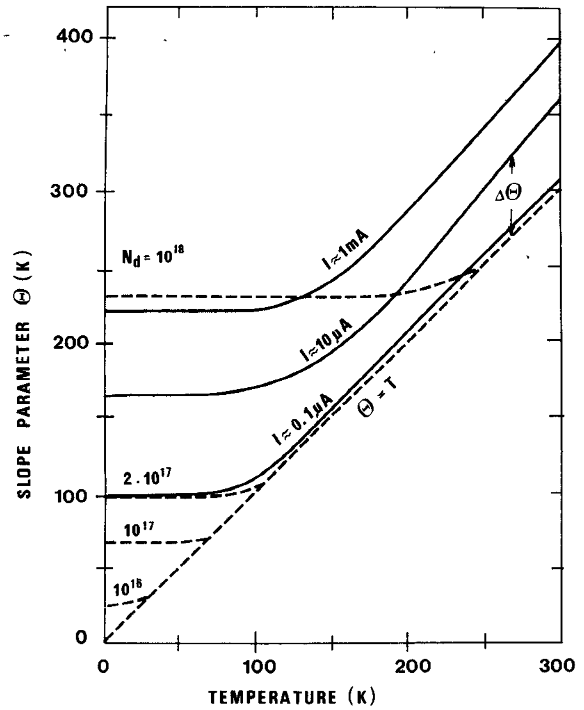

Fig. 4. The equivalent diode temperature θ as a function of diode temperature measured for $N_d = 2\cdot 10^{17}$ and calculated for different N_d (dotted lines).

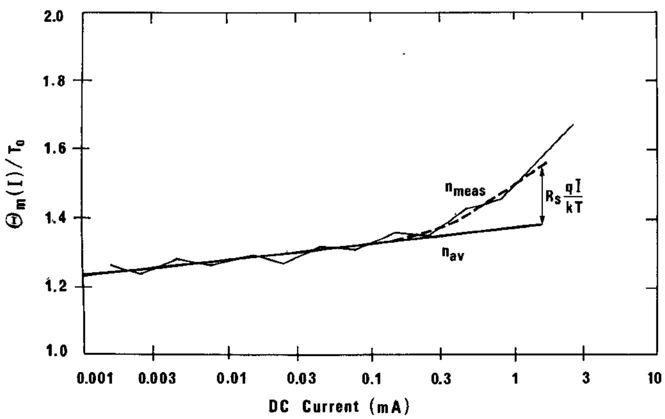

Fig. 5. Current dependence of the slope of the log $I-V$ characteristic of the diode at room temperature.

higher currents, the voltage drop across the series resistance R_s has to be taken into account. The measured value of the slope parameter $\theta_m(I)$ becomes

$$\theta_m(I) = \frac{qI}{k}\frac{\partial(V_j + IR_s)}{\partial I} = \frac{qI}{k}\left\{\frac{\partial V_j}{\partial I} + R_s\right\} \tag{4}$$

where R_s is assumed constant.

The term $(qI/k)(\partial V_j/\partial I)$ above is identical to θ, and (4) becomes

$$\theta_m(I) = \theta(I) + \frac{qI}{k}R_s. \tag{5}$$

As long as the electron temperature remains close to the device temperature T_0, and the bias voltage remains smaller than the flat-band voltage V_F ($V_F = \phi_b - V_n$), where qV_n is the distance between the bottom of the conduction band and the Fermi level in the undepleted epilayer (Fig. 3)), it can be assumed that the $\theta(I)$ relationship does not change significantly and the series resistance R_s can be determined from the relation

$$R_s = \frac{k}{qI}\left[\theta_m(I) - \theta(I)\right]. \tag{6}$$

The determination of R_s is shown graphically in Fig. 5.

Some possible causes for the linear increase of θ with current are:

1) the image force;
2) insulating layer at the metal–semiconductor interface;
3) contribution to the diode current from other transport mechanisms such as diffusion, tunneling, trapping of electrons, and recombination; and
4) distribution of spatial inhomogeneities of the barrier height discussed in [1].

Formulas were derived [11] showing that the existence of an interfacial layer at the metal–semiconductor junction, together with the image force, leads to an increase of the barrier height with the applied forward bias. In (1), this is equivalent to an increase of θ with current [26]. The relatively low donor concentration in the epilayers of investigated diodes indicates that the effects of the image force can be neglected and that only the other possible causes listed above can be responsible for the observed slow increase of θ with diode current.

Consequently, proper values of $\theta(I)$ and R_s have to be inserted into the formulas in section IV for a precise noise-temperature calculation, even in the range of small currents.

IV. Equivalent Noise Temperature of the DC-Biased Diode

The equivalent circuit of the Schottky diode is also presented in Fig. 3. The series resistance R_s represents the contacts (R_{sc}), substrate (R_{ss}), and the undepleted part of the epilayer (R_{se}), i.e., region I in Fig. 3. The junction resistance R_j and the capacitance C_j represent the interface and the depleted part of the epilayer (region II). The noise generators e_s and i_j represent the respective noise sources in these regions. Within the classical model, when electron temperature is assumed to be equal to the ambient temperature T_0 and only thermal noise is taken into account in region I and shot noise in region II, $e_s^2 = 4kT_0R_s\Delta f$ and $i_j^2 = 2qI\Delta f$. The equivalent noise temperature of the diode is then

$$T_n = \frac{1}{4k\Delta f}\frac{\dfrac{|i_j|^2R_j^2}{1+(\omega\tau_j)^2} + |e_s|^2}{\dfrac{R_j}{1+(\omega\tau_j)^2} + R_s}. \tag{7}$$

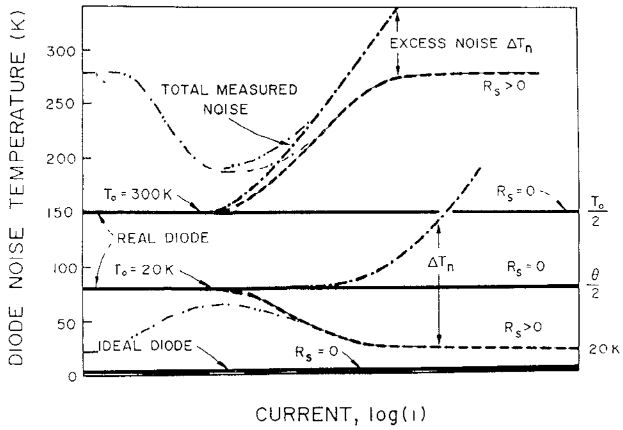

Fig. 6. Equivalent diode noise temperature. —— predicted by formula (8) for $R_s = 0$. --- predicted by (8) for $R_s > 0$ (low-frequency case). -·-·- measured. ······ predicted by (8) for $R_s > 0$ (high-frequency case).

Inserting values for $|i_j|^2$ and $|e_s|^2$, one obtains

$$T_n = \frac{R_j\theta/2 + R_s T_0\left[1+(\omega\tau_j)^2\right]}{R_j + R_s\left[1+(\omega\tau_j)^2\right]} = \frac{R_j\theta/2 + R_s T_0\left[1+\left(\frac{\omega}{\omega_j}\right)^2\right]}{R_j + R_s\left[1+\left(\frac{\omega}{\omega_j}\right)^2\right]}. \tag{8}$$

In these equations, the bias-dependent junction time constant τ_j, the junction cutoff frequency ω_j, and the junction resistance R_j are defined by the relations

$$\omega_j = \frac{1}{\tau_j} = \frac{1}{R_j C_j} \tag{9}$$

$$R_j = \frac{k\theta}{qI} = \frac{dV_j}{dI}. \tag{10}$$

Let us first discuss the case when the term $(\omega/\omega_j)^2$ is important. This occurs when

$$\frac{R_s}{R_j}\left(\frac{\omega}{\omega_j}\right)^2 = R_s R_j C_j^2 \omega^2 \to 1. \tag{11}$$

Hence, for low enough bias currents, when R_j is very large, the noise temperature T_n will approach T_0 even at quite low frequencies (say 1 GHz). This phenomenon is shown in Fig. 6 in a curve for a room-temperature diode which starts out at T_0 at low bias and then has a minimum before it goes up again at higher bias levels. For a typical millimeter-wave diode with, e.g., $C_0 \approx 8$ fF and $R_s \approx 8\ \Omega$, and for bias currents above a few microamperes, this type of behavior first becomes important when the frequency approaches 100 GHz [28].

For the typical millimeter-wave diode (see above), the noise temperature for bias currents above about 10 μA and frequencies below 50 GHz can be approximated using (8) accordingly

$$T_n = \frac{R_j\theta/2 + R_s T_0}{R_j + R_s} = \frac{\theta/2 + T_0\dfrac{qR_s}{k\theta}I}{1 + \dfrac{qR_s}{k\theta}I}. \tag{12}$$

This is the well-known Viola–Mattauch formula [12]. The first term in the numerator is caused by shot noise, while the second term is the thermal noise of the series resistance R_s. Equation (12) shows that for small currents the effective noise temperature becomes $T_n = \theta/2$, and it predicts that the second term should become dominant at large forward currents, giving $T_n = T_0$, as illustrated in Fig. 6. However, a decrease of T_n with increasing current at low temperatures when $T_0 < \theta/2$ was never reported. Instead, the measurements showed a sharp increase of the diode noise temperature T_n above a critical forward current. Thus, the total measured noise shown by the dash–dot curves in Fig. 6 for $T_0 = 300$ K and 20 K was always substantially larger at high currents than the value predicted from (12). The noise-temperature measurements showed also that the excess noise, mentioned above, is frequency dependent (Figs. 7–9). In many of the measured diodes, the excess noise strongly decreases in the frequency range 0.1–10 GHz and around 80 GHz [3]–[6].

We postulate that the excess noise ΔT_n shown in Fig. 6 is caused by excess fluctuations of the number and velocity of electrons traversing the diode.

There are two possible mechanisms producing electron velocity fluctuations in excess of those causing thermal noise corresponding to the ambient temperature (see Appendix I). The first is generation of hot electrons. These hot carriers appear if the high electric field in the undepleted epilayer accelerates the electrons to energies which exceed significantly the energy corresponding to thermal equilibrium (lattice temperature) [1], [4], [5], [8], [20]. The other is local heating of the junction caused by high current densities [15]. Mechanisms producing fluctuations of the number of electrons (electron density fluctuations) in excess of those corresponding to the shot noise (see Appendix II) are attributed to intervalley scattering; i.e. the hottest electrons are injected into a different regime of the conduction band, where they become nearly immobile because of their higher effective mass [8], [16]. These mechanisms are also attributed to generation–recombination and trapping of electrons in the undepleted epilayer and in the vicinity of the metal–semiconductor interface [7]–[10].

The total excess noise generated in the undepleted epilayer of the diode is due to the contribution of hot electrons (T_h), traps (T_{tr}), and intervalley scattering (T_{iv}) and must be included in the noise generator e_s. Since these mechanisms are independent, the total excess noise temperature, T_E in the undepleted epilayer can be written as

$$T_E = T_h + T_{tr} + T_{iv} - T_0 \tag{13}$$

$$T_E = T_0\left(\sum_1^3 \delta_n E^n\right) = T_0\left(\sum_1^3 k_n I^n\right) \tag{14}$$

with

$$k_n = k_{n(h)} + k_{n(iv)} + k_{n(tr)}$$
$$\delta_n = \delta_{n(h)} + \delta_{n(iv)} + \delta_{n(tr)} \tag{15}$$

which are frequency dependent.

The measurements of Mattauch [23] in GaAs n^+nn^+ structures yield the following values of δ parameters: $\delta_1 = (4.13/E_{th})\cdot 10^{-2}$, $\delta_2 = 1.68/E_{th}^2$, and $\delta_3 = 6.61/E_{th}^3$, where $E_{th} = 3.2$ kV/cm is the threshold field of GaAs.

Taking into account the excess noise sources and the current dependence of the slope parameter $\theta(I)$ discussed above, a more general expression for the diode noise temperature is obtained from (7)

$$T_n = \frac{R_j \frac{\theta}{2}\left(1 + \frac{S_{nJ}}{2qN_D^2V^2}I\right) + T_0\left[R_{se}\left(1 + \sum_n k_n I^n\right) + R_{sc} + R_{ss}\right]\left(1 + (\omega\tau_j)^2\right)}{R_j + R_s\left(1 + (\omega\tau_j)^2\right)}. \tag{16}$$

In the first term, representing noise generated in the barrier, besides the shot noise, noise from traps at the interface and in the depleted part of the epilayer is included and the second term is augmented by the excess noise generated in the undepleted epilayer.

The dependence of the noise temperature upon diode current can be determined by replacing R_j and τ_j with their values given by (10) and (9). If R_{sc} and R_{ss} can be neglected, $R_s = R_{se}$ and (16) becomes

$$T_n = \frac{\frac{\theta}{2}\left(1 + \frac{S_{nJ}I}{2qN_D^2V^2}\right) + T_0\frac{qR_s}{k\theta}I\left(1 + \sum_n k_n I^n\right)\left[1 + \left(\frac{\omega}{\omega_c}\frac{k\theta}{qR_sI}\right)^2\right]}{1 + \frac{qR_s}{k\theta}I\left[1 + \left(\frac{\omega}{\omega_c}\frac{k\theta}{qR_sI}\right)^2\right]}. \tag{17}$$

In the low-frequency range ($\omega \ll \omega_c$), $R_s/R_j = qI/C_jk\theta$ and for very low currents, when all terms multiplied by I can be neglected, we obtain, using (3),

$$T_n \simeq \frac{\theta}{2} = \frac{\theta_0}{2}\left[1 + \frac{\theta_1(I)}{\theta_0}\right]. \tag{18}$$

For high currents, $I \gg k/qR_s\theta$, eq. (17) for the diode noise temperature becomes

$$T_n \simeq T_0\left(1 + \sum_n k_n I^n\right) + \left(\frac{\theta}{2qN_D}\right)^2 \frac{k \cdot S_{nJ}}{V^2R_s}. \tag{19}$$

At high frequencies ($\omega \approx \omega_c$), the current dependence of the diode noise temperature becomes different, because the noise from the undepleted epilayer determines the diode noise temperature not only for high currents but also for very small currents, when $\omega\tau \gg 1$, as discussed above. Therefore, in this frequency range, the diode noise temperature at room temperature may have a minimum, and at low temperatures a diode noise temperature lower than $\theta/2$ may be measured, as shown in Fig. 6.

The contribution of the trapping noise from the interface decreases with frequency. From (16) and (A6) for $R_s \gg R_j$, one gets a contribution to the total noise from the interface traps according to

$$T_{n_{trt}} = \left(\frac{\theta}{2qN_D}\right)^2 \frac{k\alpha N_T}{VR_s} \frac{\tau}{1 + (\omega\tau)^2} \cdot \frac{1}{1 + (\omega\tau_j)^2} \tag{20}$$

where τ is the time constant related to the trapping process and $\tau_j = R_jC_j$ is the current-dependent junction time constant. For high currents, when $\omega\tau_j \ll 1$ ($I \gg (\omega/\omega_c)(k\theta/qR_s)$), eq. (16) for the diode noise temperature becomes

$$T_n = T_0\left(1 + \sum_n k_n I^n\right) \tag{21}$$

and only noise generated in the undepleted epilayer (thermal and excess) will be measured.

V. Discussion

Fig. 7 shows at low currents ($I < 0.1$ mA) a linear increase of T_n with current. As the diode cutoff frequencies at zero bias are $f_{co} = 0.7$ and 1.9 THz for CTH 188 and CTH 562 diodes, respectively, the low-frequency case should be considered. The observed increase of T_n is well explained by the $\theta(I)$ relationship given by (3). However, it should be mentioned that in this current range we found that at 20 K, θ values determined from the $\log I(V)$ characteristic measured at dc were 1.5–3 times higher than determined from noise measurements. The largest ratios between them were observed for diodes with lightly doped epilayers (see Fig. 12 in [1]). This variation is possibly caused by deep traps with long time constants or phenomena related to the existence of "parallel diodes."

At higher currents, diode noise temperature is determined by the three excess noise mechanisms, i.e., trap noise, hot-electron noise, and intervalley scattering noise.

Fig. 8 shows that the noise temperature fitted from this model is in good agreement with the observed experimental data. The fitting was made using (21), (13), and (A9). The amount of frequency-dependent noise (ΔT_{tr}) was determined by subtracting the high-frequency noise ($T_n = T_h + T_{iv}$, assumed to be a white noise in the considered frequency range) from the low-frequency noise ($T_n = T_h + T_{iv} + T_{tr}$). Then, τ was determined by fitting (A9) to the measured points by the least-square method for each cur-

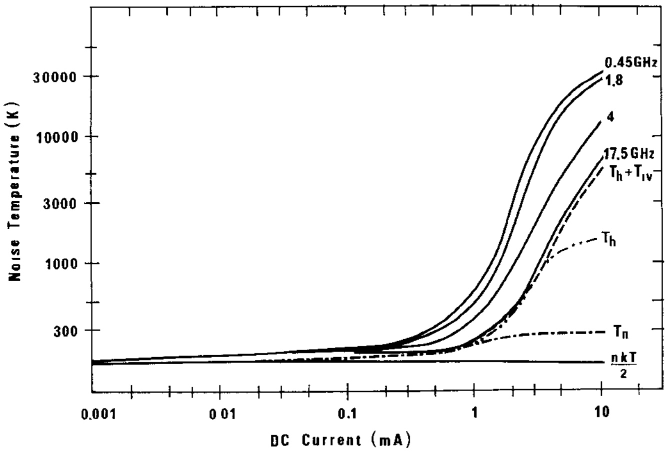

Fig. 7. Current dependence of the diode noise temperature. —— measured at different frequencies. -·-·- predicted by Viola–Mattauch formula [12]. -··-··- predicted from hot-electron temperature calculation by Maloney and Frey [18]. ---- noise temperature due to hot electrons and IV scattering from measurements after subtraction of the trap-like noise.

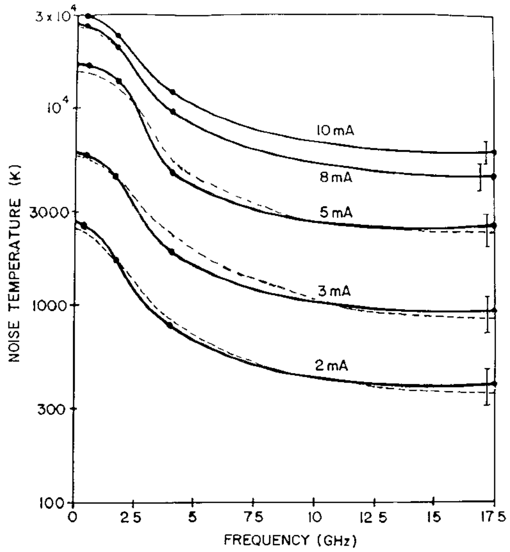

Fig. 8. Noise-temperature frequency dependence of CTH 188 diode. —— measured. ----- fitted curve assuming trap noise to dominate at low frequencies (A6) with $\tau_m = 66$ ps. estimated error of measurement.

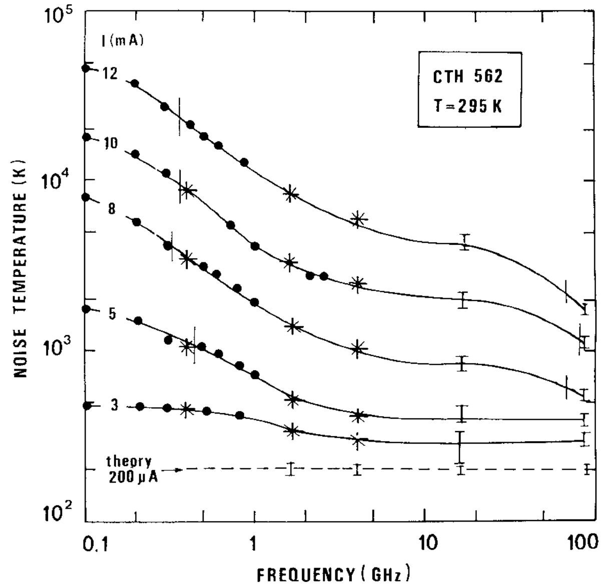

Fig. 9. Noise temperature frequency dependence of CTH 562 diode. —— noise temperature measured with mixer-receivers (I), with narrow-band amplifiers with circulators (∗), by swept measurements using a broad-band FET amplifier (●). ---- noise temperature fitted assuming trap noise to dominate at low frequencies. I frequency corresponding to time constant τ of Lorentzian distributions (see, e.g., (A6)) fitted to the experimental results.

rent. The selected final value gives the best fit for all currents.

The comparison shows that, within the experimental error, good agreement is obtained considering only one time constant $\tau \simeq 66$ ps. (We can exclude the influence of τ_j, which decreases strongly with current.) However, a number of shallow traps ($4 \cdot 10^{15}$ cm^{-3}), such as measured by Pinsard [9] and Maracas [10], can possibly account for the observed noise.

Fig. 9 shows the frequency dependence of the noise temperature for another diode. Again, a strong decrease of noise temperature is seen at frequencies below 1 GHz with an approximately Lorentzian shape given by (A9) and a time constant on the order of 450 ps.

The high-frequency measurement at 88 GHz shows a further decrease of the noise temperature. If the Lorentzian shape again is assumed, the calculated time constants for different currents are between 2 and 5 ps. This shows a reasonable agreement with the upper valley lifetime of 1.8–2 ps in GaAs and allows us to suggest that this decrease is due to the disappearance of the intervalley scattering noise according to the model discussed in Appendix II.

Further measurements of the diode noise temperature in this frequency range will give a better insight into the physics of GaAs epilayers and Schottky barriers (determination of τ_ϵ and τ_{iv}). In the analysis, other possible mechanisms affecting noise injection generation must also be included. In particular, the varying injection regime, the finite transit time, ballistic phenomena in thin epilayer structures, and quantum reflection of electrons at the metal–semiconductor interface may also be of importance.

Sometimes, rapid variations of the slope θ of the I–V diode characteristic, as shown in Fig. 4, and of noise temperature are observed. They can be modeled as being due to inhomogeneities on the diode surface and can be described by the parallel-diode model. In this case, the diode noise temperature has to be calculated as a sum of contributions of individual subdiodes. Smaller inhomogeneities will enhance some of the dependences described above, as was shown in [1].

The various noise mechanisms discussed in this paper are responsible for the large differences of the noise properties of millimeter-wave Schottky-barrier diodes. Fig. 10 shows measurements of the equivalent noise temperature of different diodes at 4 GHz as a function of current density. The comparison of the various devices shows that the excess noise can be reduced by a combination of

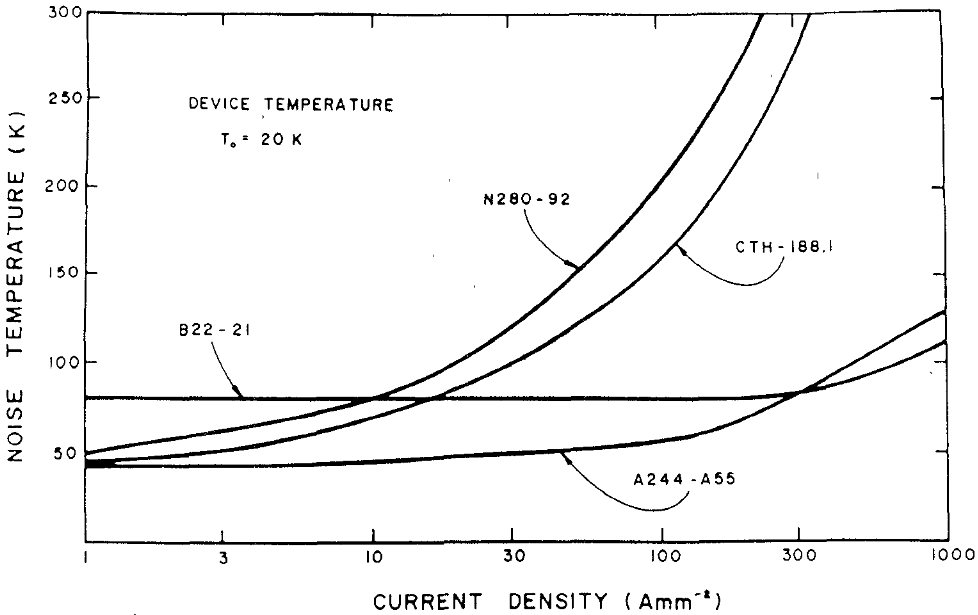

Fig. 10. Equivalent diode noise temperature as a function of current density for different device structures and fabrication techniques.

proper diode design and fabrication technology. The best performance at low and medium current densities is achieved with MBE-fabricated single-crystal Al-GaAs devices (batch A244-A55).

VI. Conclusions

We can conclude from the reported experiments that the more general formula for the equivalent noise temperature of a Schottky diode proposed here is needed to describe accurately its current and frequency dependence and to predict the noise performance of microwave and millimeter-wave mixers. The proposed more precise measurements of diode ideality factor n (or slope parameter θ) and series resistance R_s are necessary to predict accurately diode noise temperature.

An excess noise having the frequency characteristics of classical trap noise can make a significant contribution to the noise temperature of GaAs Schottky diodes. It can be reduced by using advanced growth and processing techniques for fabricating the epitaxial layer and metal–semiconductor contact. The intervalley scattering noise can be decreased by operating the junction at relatively low current densities or by choosing materials with higher intervalley energy gaps [24]. Both intervalley scattering noise and hot-electron noise [10] will be lowered if materials with higher electron mobilities at the operating point of the device can be found.

The reported results also show that, even with available diodes, mixer performances above 100 GHz can be better than those predicted from measurements at lower frequencies.

Appendix I
The Excess Electron Velocity Fluctuations

The excess electron velocity fluctuations are mainly due to the excess electron temperature, because Kerr and Held [15] showed that the local heating of the diode is not large and cannot explain the observed excess noise temperature. It has to be taken into account only to determine properly the diode series resistance. A first-order calculation of the hot-electron temperature, valid for relatively low electric fields, when the assumption of the equipartition of electron energy and their Maxwellian distribution in the undepleted epilayer is still valid, can be made on the basis of the energy balance equation. Assuming that the contributions to the diode current from gradients of carrier concentration and temperature can be neglected, one has

$$3/2nk(T_h - T_0) = \tau_\epsilon EJ \tag{A1}$$

where

T_0 ambient (lattice) temperature,
τ_ϵ energy relaxation time of electrons,
E electric field,
J diode current density,
n carrier concentration.

Utilizing the relation $J = nq\mu E$, one obtains expressions similar to those obtained in [8], [16], and [17], i.e.,

$$T_h = T_0(1+\delta_{2h}E^2) = T_0(1+k_{2h}I^2) \tag{A2}$$

with

$$\delta_{2h} = \frac{1}{T_0}\cdot\frac{2}{3}\cdot\frac{\tau_\epsilon}{k}\cdot q\mu \tag{A3}$$

$$k_{2h} = \frac{1}{T_0}\frac{2}{3}\frac{\tau_\epsilon}{k}\frac{1}{n^2 q\mu S^2} = \frac{2}{3}\frac{\tau_\epsilon}{knT_0}\frac{1}{Sd}R_{se} \tag{A4}$$

where S is the diode area, d is the thickness of the epilayer, and $R_{se} = d/nq\mu S$ is the resistance of the epilayer. The Monte Carlo simulations [18]–[20] showed, however, that $n = N_D$, τ_ϵ, and μ are constant only in a limited range of electric fields (or currents). In this range, the measurements of typical diodes give $\delta_{2h} \approx 0.1\ (\text{cm/kV})^2$ but to obtain this value from (A3), values of τ_ϵ and/or μ lower than calculated by the Monte Carlo method for a corresponding electric field [18]–[20] in bulk GaAs have to be inserted.

For a more precise evaluation, a numerical calculation of hot-electron temperatures is needed. Such a calculation performed for bulk GaAs by Frey [18] showed that due to the scattering of the hottest electrons to the low-mobility valley, the electron temperature is limited to approximately 1200 K, as shown in Fig. 7. This dependence can be described only by a polynomial of the order N higher than 2. It leads to an expression for the hot-electron temperature more general than (A2) and valid in a much wider temperature range

$$T_h = T_0\left(1 + \sum_{n=1}^{N} \delta_{nh} E^n\right) = T_0\left(1 + \sum_{n=1}^{N} k_{nh} I^n\right). \quad \text{(A5)}$$

Appendix II
Fluctuations of the Number of Electrons

The investigated diodes, even for relatively small currents for which intervalley scattering was insignificant, showed a frequency-dependent noise temperature which was also much higher than the shot noise and the hot electron temperature predicted in [18]. The observed frequency dependence is characteristic of the so-called trapping or generation–recombination noise, often described as a modulation noise [21]. If traps are at the interface or in the depleted layer, the fluctuation of their occupancy is equivalent to the fluctuation of the barrier height. If they are in the undepleted epilayer, the fluctuation of diode series resistance can be expected. Noise generated by these processes has been studied by several authors [7], [21], [22]. If the time constants τ for different processes are quite different, a binomial distribution of electrons between the conduction band and a given trap level can be assumed. Scattering by such traps causes fluctuations of the number of carriers in the conduction band whose spectral density S_n is approximately equal to the sum of contributions of different traps. The spectral density of fluctuations of the number of carriers caused by one specific type of trapping mechanism is

$$S_{nm} = \alpha N_T V \frac{\tau}{1 + (\omega\tau)^2} \quad \text{(A6)}$$

where $N_T V$ is the number of traps, V is the considered volume, τ_m is the time constant related to this trap, and α is a constant adjusted to fit the data.

The short-circuit noise current spectral intensity in the undepleted epilayer is equal to

$$S_i = (q\bar{v})^2 S_n = \frac{I^2}{n^2 \cdot V^2} S_n \quad \text{(A7)}$$

where $\bar{v}$ is the average velocity of electrons and $n \cdot V$ is their average number, equal to $N_D \cdot V$ when the diode operates in low-injection regime, with N_D being the donor density and V the volume of the undepleted epilayer.

The short-circuit noise current density S_i caused by traps in the space charge region of the Schottky diode is also proportional to I^2 (see Hsu [25]). His formulas, however, have to be modified if mechanisms other than the image force are causing the barrier height modulation.

The excess noise temperature caused by traps is calculated from the relation

$$T_{tr} = \frac{S_i}{4k} R = T_0 k_{2tr} I^2, \quad \text{with } k_{2tr} = \frac{S_n}{4kn^2V^2T_0} \cdot R \quad \text{(A8)}$$

where R is equal to R_{se} in the undepleted region and R_j in the depleted region. This temperature has to be added to the other noise sources.

For only one type of trap in the undepleted epilayer, if τ is the trap time constant in low-injection regime, (A8) becomes

$$T_{tr} = \Delta T_{tr} \frac{1}{1 + (\omega\tau)^2}. \quad \text{(A9)}$$

Comparing the contributions to the noise temperature of the undepleted epilayer from one type of trap and hot-electron noise from (A2), (A6), and (A8), one gets, with τ as a general trap time constant,

$$\frac{T_{tr}}{T_h - T_0} = \frac{3}{8} \frac{N_T}{N_D} \frac{\tau}{\tau_\epsilon} \frac{1}{1 + (\omega\tau)^2}. \quad \text{(A10)}$$

The influence of the noise due to traps as compared to hot-electron noise can be neglected if, by an appropriate diode technology, their number will be kept low enough to satisfy the relation

$$N_{T_m} \ll N_D \frac{\tau}{\tau_\epsilon}. \quad \text{(A11)}$$

At higher frequencies ($\omega \gg 1/\tau$), the trap noise disappears and the two remaining sources of excess noise, i.e., hot-electron noise and intervalley scattering noise, should dominate.

The low-mobility valley in GaAs is acting as a trap for the electrons; therefore, (16) can be applied to calculate the frequency characteristic of intervalley scattering noise temperature T_{iv}. It is generally assumed that the lifetime of electrons in the low-mobility L valley is 1.8–2 ps. Therefore, one can expect that for frequencies higher than 80 GHz the intervalley scattering noise should disappear.

Acknowledgment

The authors would like to thank C. O. Lindström for help during the measurements, and Dr. M. V. Schneider for stimulating discussions and for supplying some of the diodes investigated. They would also like to thank Dr. W. Kelly and S. Nilsen for supplying the mixer diodes.

References

[1] E. Kollberg, H. Zirath, and A. Jelenski, "Temperature variable characteristics and noise of metal–semiconductor junctions," *IEEE Trans. Microwave Theory Tech.*, vol. MTT-34, pp. 913–922, Sept. 1986.

[2] M. V. Schneider, A. Y. Cho, E. Kollberg, and H. Zirath, "Characteristics of Schottky diodes with microcluster interface," *Appl. Phys. Lett.*, vol. 43, pp. 558–560, Sept. 1983.

[3] E. Kollberg, H. Zirath, M. V. Schneider, A. Y. Cho, and A. Jelenski, "Characteristics of millimeter-wave Schottky diodes with micro-cluster interface," in *Proc. 13th European Microwave Conf.* (Nuremberg), 1983, pp. 561–566.

[4] N. J. Keen and H. Zirath, "Hot-electron generation in gallium-arsenide-Schottky-barrier diodes," *Electron. Lett.*, vol. 19, pp. 853–854, 1983.

[5] A. Jelenski, M. V. Scheider, A. Y. Cho, E. L. Kollberg, and H. Zirath, "Noise measurements and noise mechanisms in microwave mixer diodes," in *Proc. IEEE/MTT-S Int. Microwave Symp.* (San Francisco, CA), May 1984.

[6] H. Zirath, S. Nilsen, E. Kollberg, T. Andersen, and W. Kelly, "Noise in microwave and millimeter-wave Pt-GaAs Schottky diodes," in *Proc. 14th European Microwave Conf.* (Liege, Belgium), Sept. 1984.

[7] C. T. Sah, "Theory of low frequency generation noise in junction-gate field effect transistors," *Proc. IEEE*, vol. 52, pp. 795–814, July 1964.

[8] W. Baechtold, "Noise behavior of GaAs field-effect transistors with short gate lengths," *IEEE Trans. Electron Devices*, vol. ED-19, pp. 674–680, 1972.

[9] J. L. Pinsard and A. Zylbersztejn, "Microwave noise due to deep levels in GaAs MESFET's," *Inst. Phys. Conf.*, ser. no. 56, pp. 435–444, 1981.

[10] G. N. Maracas *et al.*, "Investigation of deep levels in GaAs MESFETS," in *Proc. 8th Biannual Cornell Eng. Conf.*, 1981, pp. 149–158.

[11] E. H. Rhoderick, *Metal–Semiconductor contacts* (Monographs in Electrical and Electronic Engineering). Oxford: Clarendon Press, 1980.

[12] T. J. Viola and R. J. Mattauch, "Unified theory of high frequency noise in Schottky barriers," *J. Appl. Phys.*, vol. 44, pp. 2805–2808, 1973.

[13] M. V. Schneider, R. A. Linke, and A. Y. Cho, "Low-noise millimeter-wave diodes prepared by molecular beam epitaxy (MBE)," *Appl. Phys. Lett.*, vol. 31, pp. 219–221, 1977.

[14] M. V. Schneider and M. J. Gans, "Mean distance between impurity ions in solid-state devices," *Bull. Amer. Phys. Soc.*, vol. 29, no. 4, Apr. 1984.

[15] D. N. Held and A. R. Kerr, "Conversion loss and noise of microwave and millimeter-wave mixers," *IEEE Trans. Microwave Theory Tech.*, vol. MTT-26, pp. 49–61, Feb. 1978.

[16] U. Seeger, *Semiconductor Physics.* New York: Springer Verlag, 1973.

[17] P. J. Price, "Fluctuations of hot electrons," ch. 8 in *Fluctuation Phenomena in Solids*, R. E. Burgess, Ed. New York: Academic Press, 1965.

[18] T. J. Maloney and J. Frey, "Transient and steady-state electron transport properties of GaAs and InP," *J. Appl. Phys.*, vol. 48, pp. 781–787, 1977.

[19] T. K. Glisson *et al.*, "Transient response of electron transport in GaAs using Monte Carlo method," in *VLSI Electronics: Microstructure Sciences*, vol. 4. New York: Academic Press, 1982.

[20] R. Fauquemberque, J. Zimmermann, A. Kaszynski, and E. Constant, "Diffusion and power spectral density and correlation function of velocity fluctuation for electrons in Si and GaAs by Monte Carlo methods," *J. Appl. Phys.*, vol. 51, pp. 1065–1071, 1980.

[21] R. E. Burgess, "Electronic fluctuations in semiconductors," *Brit. J. Appl. Phys.*, vol. 6, pp. 185–190, June 1955.

[22] K. M. van Vliet and J. R. Fawcett, "Fluctuations due to electronic transitions and transport in solids" in *Fluctuation Phenomena in Solids.* New York: Academic Press, 1965.

[23] R. J. Mattauch, "Local oscillator induced noise in GaAs Schottky mixer diodes," *Electron. Lett.*, vol. 13, pp. 22–23, Jan. 1977.

[24] C. Y. Chen *et al.*, "Quasi Schottky barrier diode on n- GaInAs using a fully depleted p^+-GaInAs layer grown by MBE," *Appl. Phys. Lett.*, vol. 40, pp. 401–403, Mar. 1982.

[25] S. T. Hsu, "Low frequency excess noise in metal–silicon Schottky barrier diodes," *IEEE Trans. Electron Devices*, vol. ED-17, pp. 496–506, 1970.

[26] A. Jelenski, "Accurate evaluation of the ideality factor and series resistance of millimeter-wave Schottky-barrier diodes," in *5th Annu. Benjamin Franklin Symp. Dig.*, May 4, 1985, pp. 70–72.

[27] N. J. Keen, "Low noise millimeter-wave mixer diodes: Results and evaluation of a test programme," *Proc. Inst. Elec. Eng.*, vol. 127, pt 1, no. 4, pp. 188–198, Aug. 1980.

[28] H. Zirath and E. Winberg, "A novel millimeter-wave solid state cold load," *Proc. 15th European Microwave Conf.* (Paris), 1985, pp. 293–302.

[29] G. Hegazi, A. Jelenski, and K. S. Yngvesson, "Limitations of microwave and millimeter-wave mixers due to excess noise," *IEEE Trans. Microwave Theory Tech.*, vol. MTT-33, pp. 1404–1409, 1985.

[30] A. Jelenski, E. Kollberg, M. V. Schneider, and H. Zirath, "Accurate determination of the series resistance of mm-wave Schottky diodes," in *Proc. 15th European Microwave Conf.* (Paris), 1985, pp. 279–285.

A. Jelenski (M'84) received the B.S. and M.S. degrees from the Technical University of Gdansk Poland, in 1954 and 1956, respectively, and the Ph.D. degree from the University of Paris in 1963.

From 1954 to 1969, he was engaged in research on quantum electronic devices at the Institute of Fundamental Technical Problems of the Polish Academy of Sciences. On leave from the Institute of Electron Technology CEMI in Warsaw, Poland, he is now Visiting Professor in the Department of Electrical and Computer Engineering at the University of Massachusetts, Amherst. His current research interests are the analysis, design, and characterization of microwave and millimeter-wave semiconductor devices and circuits.

Erik L. Kollberg (M'83–SM'83) was born in Stockholm, Sweden. He received the M.Sc. degree in electrical engineering in 1961, the Tekn. Licentiat degree in 1965, and the Teknologie Doktor degree in 1970, all from Chalmers University of Technology, Göteborg, Sweden.

He is now a Professor at Chalmers University of Technology and is responsible for the development of low-noise receivers for the Onsala Space Observatory. From 1963 to 1976, he worked on low-noise maser amplifiers. Since 1972, he has also been working on low-noise millimeter-wave mixers. These mixers have been used for radio astronomy observations at Onsala since 1979. More recently, he has been working on extremely low-noise superconducting (quasiparticle) mixers, and experimental receivers are now in use at the Onsala Observatory. He and his coworkers have also started development work on GaAs millimeter-wave components.

Dr. Kollberg is Chairman of the Microwave Theory and Techniques Chapter of the IEEE Swedish Section. He is also a member of the Swedish branch of URSI.

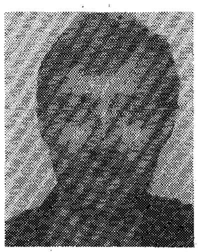

Herbert H. G. Zirath was born in Göteborg, Sweden, on March 20, 1955. He received the M.Sc. degree in 1980 from Chalmers University of Technology, Göteborg, Sweden.

Since 1980, he has been working as a Research Assistant at Chalmers University of Technology on cooled millimeter-wave Schottky mixers and on the properties of millimeter-wave Schottky-barrier diodes including current transport and high-frequency noise generation. Mr. Zirath is currently working toward the Ph.D. degree in electrical engineering at Chalmers University of Technology.